

1
2
3
4
5
6
7
8
9
10
11
12
13
14
15
16
17

Electronic Supplementary Information

Directly Electro-Catalyze Crude Syngas to Ethylene via a Multi- Process Coupled Device

Mo Zhang,^{ab} Ruixue Chen,^b Suheng Wang,^b Yunchuan Tu,^a Xiaoju Cui,^{*ac} Dehui
Deng^{*abc}

^a State Key Laboratory of Catalysis, Collaborative Innovation Center of Chemistry for Energy
Materials, Dalian Institute of Chemical Physics, Chinese Academy of Science, Dalian 116023,
China.

^b State Key Laboratory of Physical Chemistry of Solid Surfaces, Collaborative Innovation Center of
Chemistry for Energy Materials, College of Chemistry and Chemical Engineering, Xiamen
University, Xiamen 361005, China.

^c University of Chinese Academy of Sciences, Beijing 100049, China.

* Email: cuixiaoju@dicp.ac.cn, dhdeng@dicp.ac.cn

18 **Experimental Section**

19

20 **Chemicals**

21 $\text{Co}(\text{NO}_3)_3 \cdot 6\text{H}_2\text{O}$, $\text{Ni}(\text{CH}_3\text{COO})_2 \cdot 4\text{H}_2\text{O}$, urea, citric acid and ethylene glycol (99.8%)
22 were purchased from Sigma-Aldrich. $\text{CuSO}_4 \cdot 5\text{H}_2\text{O}$, L-ascorbic acid, ethanol, NaOH,
23 NaCl and polyvinyl pyrrolidone K-30 (PVP) were purchased from Sinopharm
24 Chemical Reagent Co., Ltd. $\text{Na}_2\text{S} \cdot 6\text{H}_2\text{O}$ were purchased from Xilong Scientific Co.,
25 Ltd. All chemicals were used as received without further purification.

26

27 **Preparation of CoNi@NGs and CoNiO_x-CNTs**

28 The CoNi@NGs were prepared through a template-assisted method.¹ Briefly, Co
29 and Ni precursor were precipitated on the SiO_2 templet by the hydrothermal method.
30 Then transfer the gotten sample into a CVD furnace, and deposit graphene shells by
31 bubbling CH_3CN as the carbon and nitrogen source at 600 °C. Finally, the samples
32 CoNi@NGs were collected after washed in HF aqueous solution and distilled water.
33 For CoNiO_x-CNTs preparation, the Co and Ni precursor were firstly precipitated on the
34 carbon nanotubes (CNTs) via the hydrothermal method, and then the sample was treated
35 at 400 °C under Ar for 1 h in the CVD furnace.

36

37 **Preparation of Cu catalyst**

38 For synthesis of Cu catalyst, $\text{CuSO}_4 \cdot 5\text{H}_2\text{O}$, PVP and NaCl were dissolved by
39 ethylene glycol (EG) in a flask. Then the mixture of NaOH and L-ascorbic acid EG
40 solution was preheated was injected to the flask for 40 minutes in the heating of 100 °C.
41 The Cu catalyst was collected by centrifuge and washed with deionized H_2O and
42 ethanol, respectively. The obtained Cu sample was dispersed into ethanol and used for
43 preparing cathodic electrode for CO electroreduction.²

44

45 **Characterization**

46 Transmission electron microscope (TEM) was conducted on Tecnai F20

47 transmission electron microscope operated at an accelerating voltage of 200 kV.
48 Scanning electron microscopy (SEM) measurements were carried out by using Hitachi
49 S-4800 scanning electron microscope with 15 kV accelerating voltage. The Faradic
50 efficiency (FE) of gas phase products was measured on gas chromatography GC 2060
51 produced by Ruimin Instrument Company in Shanghai. The FE of liquid phase products
52 was analyzed on a Bruke 500-MHz NMR spectrometer. The content of H₂S was
53 confirmed by Quadrupole Mass Spectrometer EQMS-I (Shanghai Quan Tang Scientific
54 Instruments).

55

56 **Electrochemical measurements**

57 All the electrochemical measurements were carried out with CHI 760E equipped
58 with a gas flow controlling system at 25 °C. The test was carried in a double-cell
59 electrolytic tank segregated with Nafion 117 membrane. The electrodes were set in the
60 1 M NaOH electrolyte.

61

62 **Preparation of the anodic electrode**

63 The anodic electrode was assembled by covering CoNi@NGs catalyst on a Ni
64 foam electrode (1 cm² square, 1 mm thickness). Typically, 7 mg CoNi@NGs catalyst
65 was dispersed in 1.95 mL ethanol with 50 uL Nafion solution (5 wt%, Du Pont) to form
66 a homogeneous ink. Then 2 mL ink was added dropwise onto the Ni foam and dried
67 under the room temperature. The final loading of CoNi@NGs was 7 mg cm⁻².

68

69 **Preparation of the cathodic electrode**

70 The carbon paper (GDS3250) with micro-porous layer (MPL) was bought from
71 *AvCarb Material Solutions*. For preparing electrode loading catalysts, 10 mg catalysts
72 and 50 μL Nafion solution were dispersed into 1.5 mL ethanol by ultrasound. Then the
73 ink was dropped on the carbon papers and dried under the room temperature. The final
74 loading of Cu particles was 1 mg cm⁻².

75

76 **The SOR catalytic performance test of CoNi@NGs**

77 For SOR reaction, 1 M Na₂S was added in the anodic electrolyte. The polarization
78 curve of CoNi@NGs was tested in a standard three-electrode cell. The reference
79 electrode Hg/HgO was calibrated according to the formula $E_{\text{versus RHE}} = 0.098 + 0.0591$
80 pH. The pH was tested by the pH value meter at 25 °C. The activities of CoNi@NGs
81 were evaluated with a scan rate of 5 mV/s. The test of galvanostatic method was tested
82 in a standard two-electrode cell. The catalytic performance of direct electrolysis of H₂S-
83 contained syngas was performed after bubbling the H₂S-contained syngas to the anodic
84 electrolyte for one hour.

85

86 **The CORR catalytic performance of Cu catalyst**

87 The performance of Cu catalyst in the coupled device was measured by the
88 galvanostatic method. The FE of gas phase and liquid phase products was measured by
89 gas chromatography and NMR spectrometer, respectively.

90

91 **Gas chromatography and NMR analysis**

92 The amount of H₂ and C₂H₄ was evaluated by gas chromatography. During the test,
93 reaction gas (CO or syngas) was purged continuously through the mass flow meter and
94 directly routed into gas chromatography every 10 min. Quantification of the H₂ and
95 C₂H₄ were performed using the thermal conductivity detector (TCD) and flame
96 ionization detector (FID), respectively. The quantity and retention time of the gas were
97 calibrated with a series of standard gas samples. The FEs of cathodic gas products were
98 calculated by the following equation:

99
$$R_{\text{product}} = \frac{A_{\text{test}}}{A_{\text{standard}}} \times c_{\text{standard}} \times R_{\text{reaction gas}}$$

100
$$i_{\text{product}} = R_{\text{product}} \times \frac{2Fp_0}{RT}$$

101
$$FE_{\text{product}} = \frac{i_{\text{product}}}{i_{\text{total}}} \times 100\%$$

102 R_{product} : flow rate of H₂ or C₂H₄

103 A_{test} : peak area of the gas generated at the specific time point

- 104 $A_{standard}$: peak area of the gas in the standard gas samples
 105 $c_{standard}$: volume concentration of test gas in the standard gas samples
 106 $R_{reaction\ gas}$: flow rate of reaction gas
 107 $i_{product}$: geometric current density of H₂ or C₂H₄
 108 F : Faradic constant, 96485 C mol⁻¹
 109 p_0 : pressure
 110 R : ideal gas constant, 8.314 J mol⁻¹ K⁻¹
 111 T : temperature, 298 K
 112 $FE_{product}$: Faradic efficiency of H₂ or C₂H₄
 113 i_{total} : total current density in the reaction

114 The liquid products were analyzed on a Bruke 500-MHz NMR spectrometer. The
 115 0.5 mL sample of the electrolyte was mixed with 0.05 mL D₂O and 0.05 mL 2.38 mM
 116 dimethyl sulphoxide (DMSO, used as internal standard). The one-dimensional ¹H
 117 spectrum was measured with water suppression method. The amount of products were
 118 calculated according to standard curves, which were tested by a series of standard gas
 119 samples.

120 There are four carbon-based products in the cathode from CORR. The selectivity
 121 of C₂H₄ was were calculated by the following equation:

$$122 \quad FE_{CORR} = FE_{C_2H_4} + FE_{EtOH} + FE_{AcO^-} + FE_{n-Pro}$$

$$123 \quad S_{C_2H_4} = \frac{FE_{C_2H_4}}{FE_{CORR}}$$

124 FE_{CORR} : The cathodic FE of CO reduced reaction

125 $S_{C_2H_4}$: The selectivity of C₂H₄

126

127 **Energy saving efficiency analysis**

128 The value of energy saving efficiency was calculated to verify the low energy
 129 consumption of ethylene production in the coupled device versus uncoupled device.

130 The energy saving efficiency is calculated based on the following equations:

$$131 \quad E_{device} = U \times I \times t$$

132
$$E_u \text{ or } E_c = \frac{E_{device} \times F E_{C_2H_4}}{n_{C_2H_4}}$$

133
$$\text{Energy Saving efficiency}_{C_2H_4} = \frac{E_u - E_c}{E_u} \times 100\%$$

134 E_{device} : the energy consumption of the device

135 U : the applied potential for the device

136 I : the applied current for the device

137 t : reaction time

138 $E_u \text{ or } E_c$: the energy consumption of ethylene production in the uncoupled device (E_u)

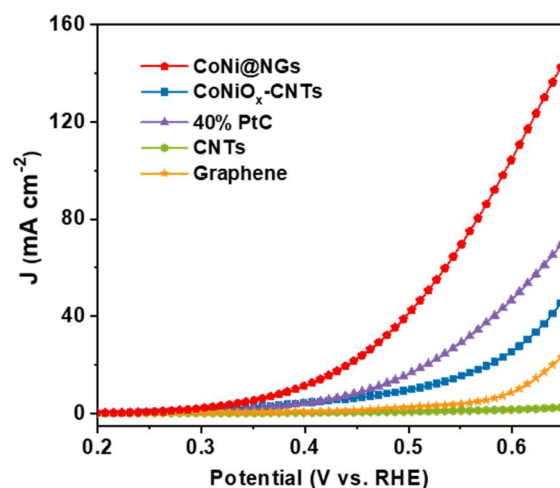
139 or coupled device (E_c)

140 $n_{C_2H_4}$: the amount of produced C_2H_4

141 $\text{Energy Saving efficiency}_{C_2H_4}$: the energy saving efficiency in the multi-process

142 coupled device

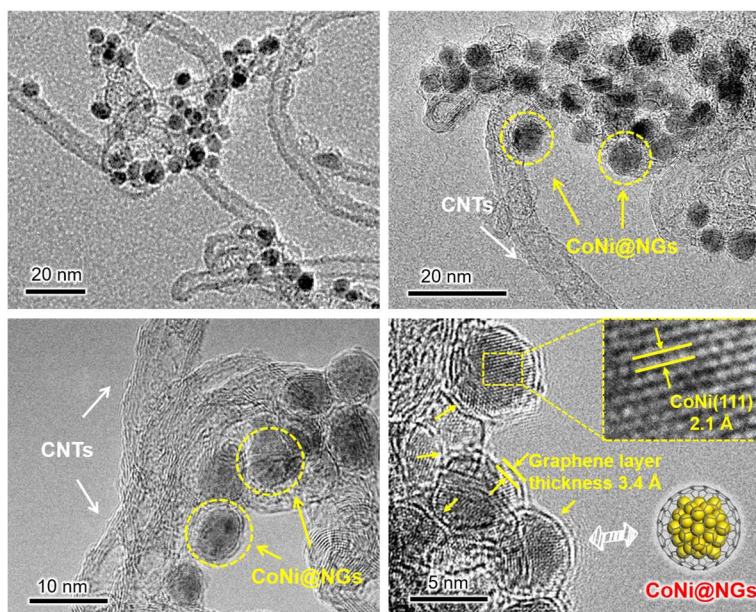
143



144

145 **Fig. S1** The SOR polarization curves for CoNi@NGs in comparison with 40% Pt/C,
 146 graphene, carbon nanotubes (CNTs) and the cobalt and nickel oxide nanoparticles
 147 supported on carbon nanotubes (CoNiO_x-CNTs) at the same mass loading. The current
 148 density of CoNi@NGs is much higher than the other materials, which indicates that
 149 CoNi@NGs possess a higher activity for H₂S oxidation. The mixture of 1 M NaOH and
 150 1 M Na₂S serves as the anodic electrolyte and 1 M NaOH serves as the cathodic
 151 electrolyte.

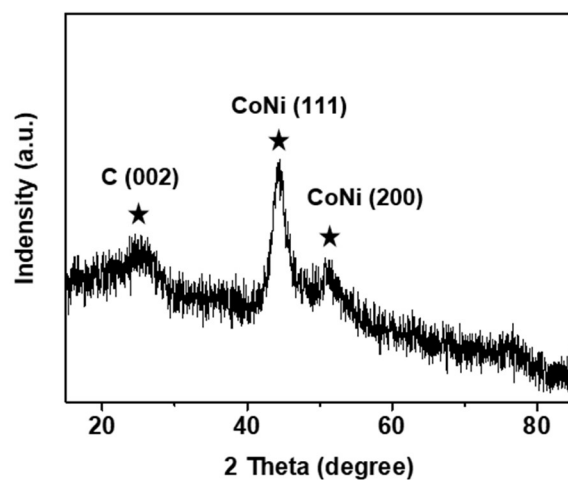
152



153

154 **Fig. S2** The TEM images of CoNi@NGs. It clearly shows that the CoNi alloy
 155 nanoparticles are encapsulated by the single layer graphene.

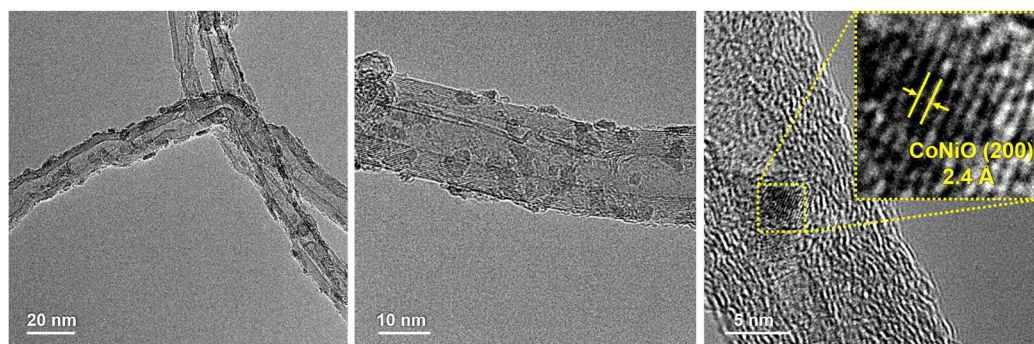
156



157

158 **Fig. S3** The X-ray diffraction (XRD) pattern of CoNi@NGs. The crystal structure of
 159 CoNi alloy NPs is confirmed by the XRD test, which exhibits two main diffraction
 160 peaks at $2\theta = 44.44^\circ$, and 51.72° , corresponding to the (111) and (200) facets of the
 161 CoNi alloy.

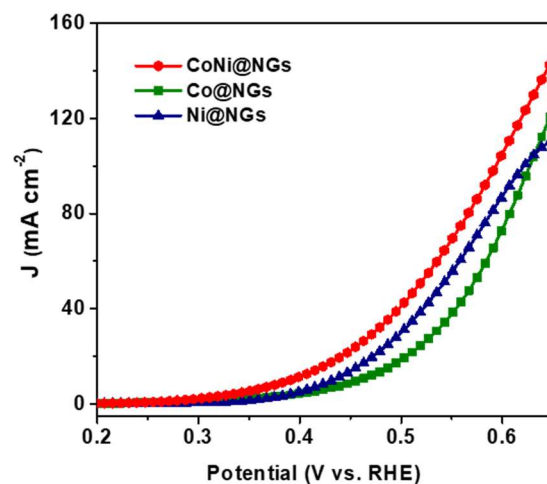
162



163

164 **Fig. S4** The HRTEM images of CoNiO_x-CNTs. The cobalt and nickel oxide
 165 nanoparticles (CoNiO_x) are supported on the CNTs evidenced by the crystal plane of
 166 CoNiO(200).

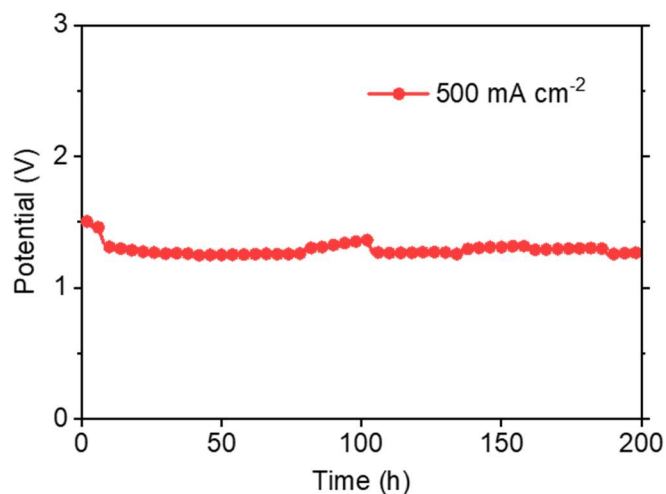
167



168

169 **Fig. S5** The SOR polarization curves for CoNi@NGs in comparison with Co@NGs,
 170 Ni@NGs at the same mass loading. The current density of CoNi@NGs is much higher
 171 than the Co@NGs and Ni@NGs. The mixture of 1 M NaOH and 1 M Na₂S serves as
 172 the anodic electrolyte and 1 M NaOH serves as the cathodic electrolyte.

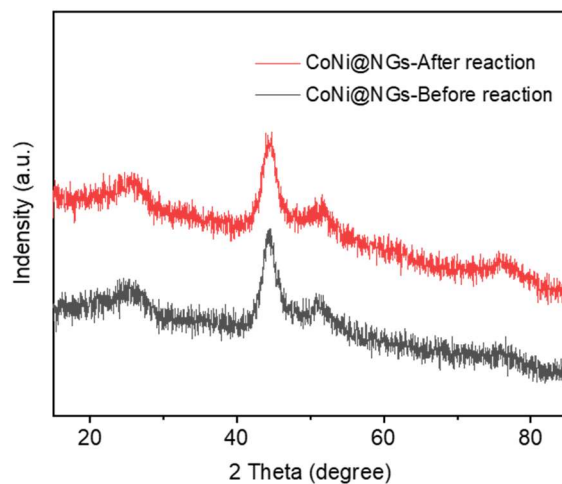
173



174

175 **Fig. S6** Galvanostatic test for the CoNi@NGs in the SOR at the current density of 500
 176 mA cm⁻² for 200 hours.

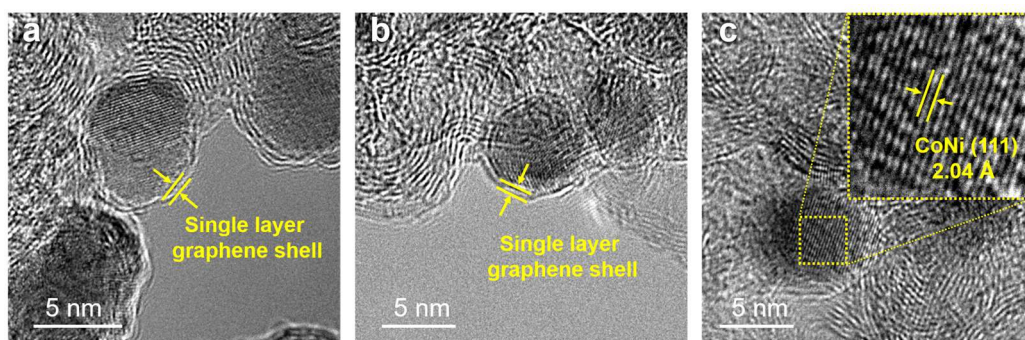
177



178

179 **Fig. S7** The X-ray diffraction (XRD) pattern of CoNi@NGs before and after 200 hours'
 180 durability test.

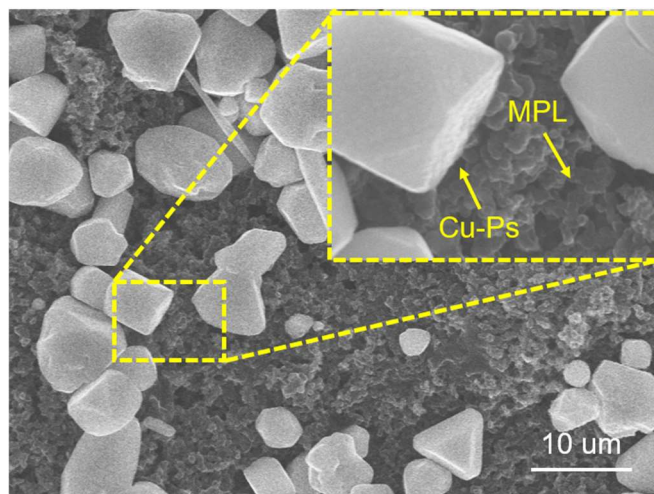
181



182

183 **Fig. S8** The HRTEM images of CoNi@NGs after 200 hours' durability test.

184

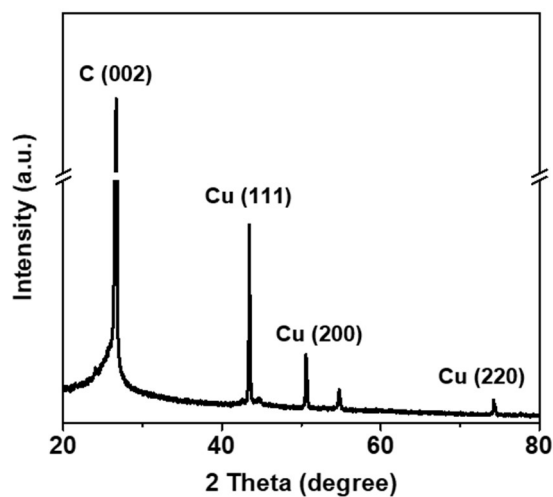


185

186 **Fig. S9** The SEM image of Cu catalyst electrode. The Cu particles were loaded on the
 187 carbon paper with micro-porous layer.

188

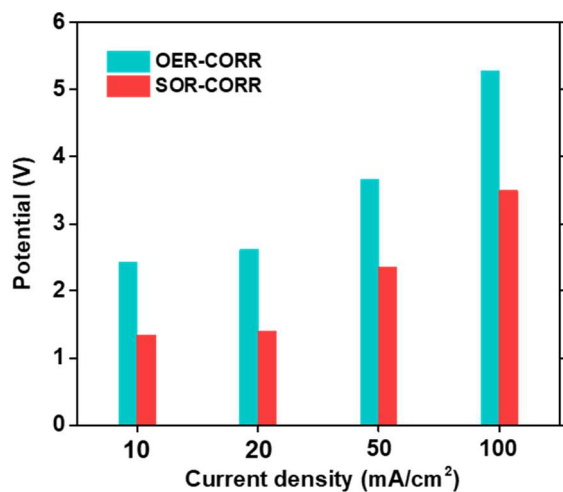
189



190

191 **Fig. S10** The XRD pattern of Cu catalyst. The crystal structure of Cu presents three
 192 main diffraction peaks, corresponding to the (111), (200) and (220) facets of the Cu foil.

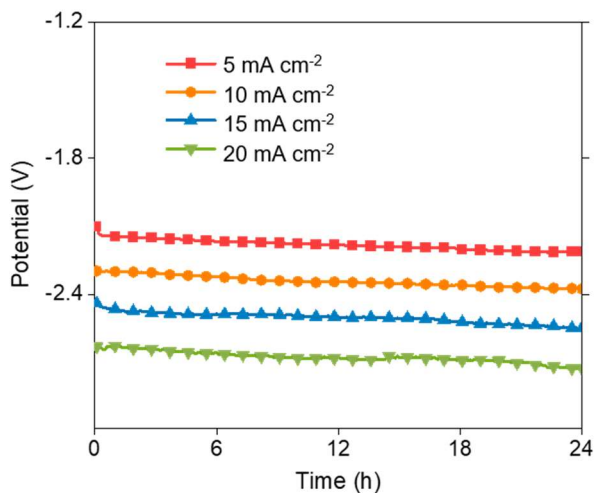
193



194

195 **Fig. S11** Comparison of the potentials for SOR-CORR and OER-CORR at the current
 196 density of 10, 20, 50 and 100 mA cm⁻².

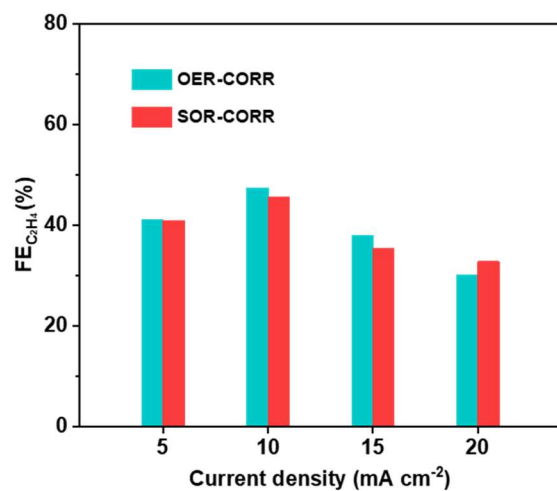
197



198

199 **Fig. S12** Galvanostatic test for the uncoupled device in the OER-CORR process at the
 200 current density from 5 to 20 mA cm⁻² in 24 hours.

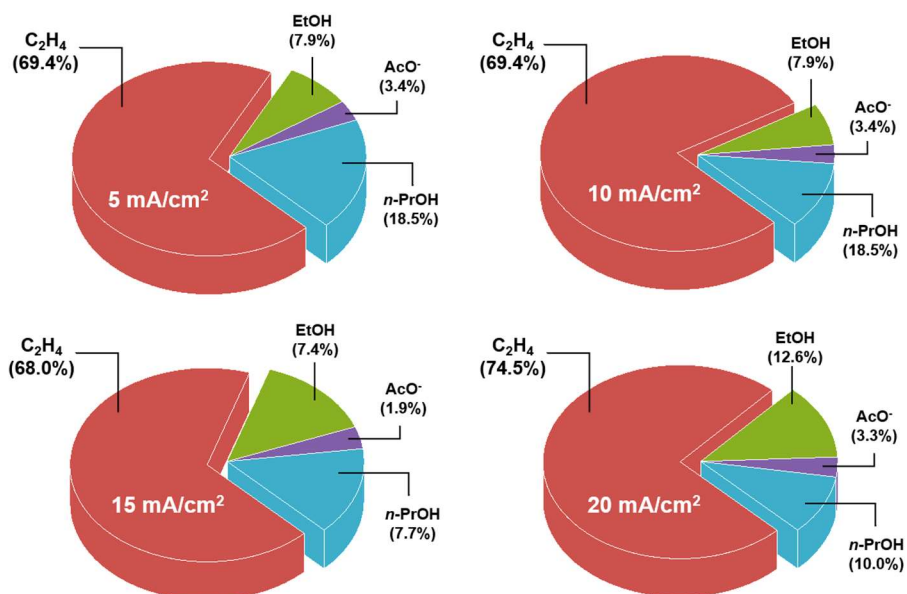
201



202

203 **Fig. S13** The comparison of FE for ethylene production in the SOR-CORR process and
 204 the OER-CORR process.

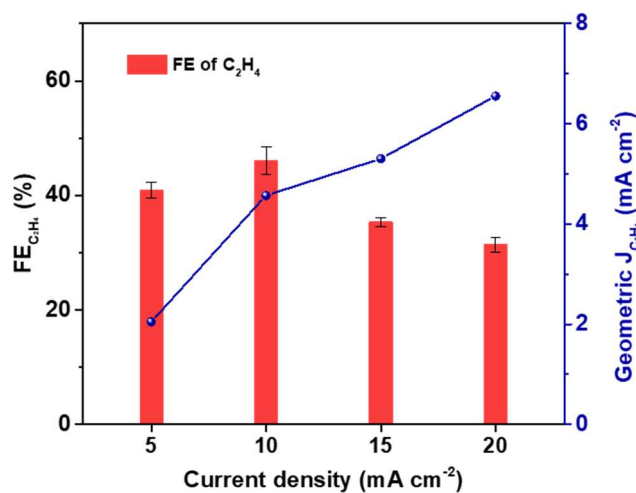
205



206

207 **Fig. S14** The selectivity of CORR at the current density from 5 to 20 mA cm⁻².

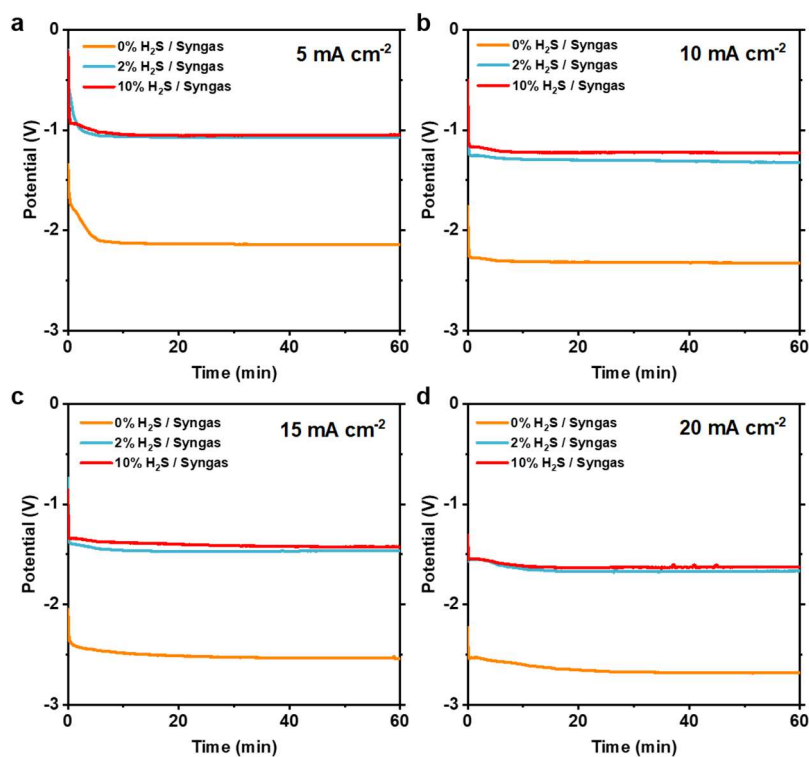
208



209

210 **Fig. S15** The geometric current density for CO electroreduction to C₂H₄ production in
 211 the two-electrode SOR-CORR reaction.

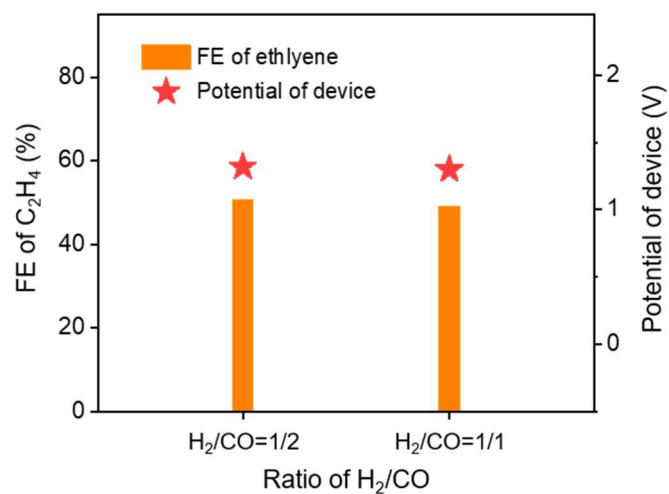
212



213

214 **Fig. S16** The potentials of the coupled device at different current densities when dealing
 215 with different syngas.

216



217

218 **Fig. S17** The effect of different ratio of H₂ to CO on the performance of direct
 219 electrolysis of crude syngas containing 2% H₂S.

220

221 **Table S1.** The FE of CORR products at the cathode when dealing with 0% H₂S-
 222 contained syngas with 1 M NaOH as electrolyte.

223

Current density (mA cm ⁻²)	FE of products (%)				Selectivity of ethylene (%)
	C ₂ H ₄	EtOH	AcO ⁻	<i>n</i> -PrOH	
5	41.6	7.9	2.0	14.4	63.1
10	50.2	8.9	1.1	8.2	73.4
15	39.0	6.0	1.9	5.9	73.9
20	25.9	6.8	0.8	3.7	69.6

224

225

226

227 **Table S2.** The FE of CORR products at the cathode when dealing with 2% H₂S-
 228 contained syngas with 1 M NaOH as electrolyte.

229

Current density (mA cm ⁻²)	FE of products (%)				Selectivity of ethylene (%)
	C ₂ H ₄	EtOH	AcO ⁻	<i>n</i> -PrOH	
5	41.1	3.7	1.7	13.4	68.6
10	50.6	6.8	1.1	7.0	77.3
15	37.8	8.2	2.1	6.2	69.6
20	25.4	6.7	1.0	6.6	64.0

230

231

232

233

234 **Table S3.** The FE of CORR products at the cathode when dealing with 10% H₂S-
235 contained syngas with 1 M NaOH as electrolyte.

236

Current density (mA cm ⁻²)	FE of products (%)				Selectivity of ethylene (%)
	C ₂ H ₄	EtOH	AcO ⁻	<i>n</i> -PrOH	
5	40.6	10.0	2.8	12.2	61.9
10	49.7	8.4	1.0	7.2	75.0
15	38.5	7.7	0.9	6.6	71.7
20	25.7	6.1	1.1	4.2	69.3

237

238

239 **References**

240

241 1 M. Zhang, J. Guan, Y. Tu, S. Chen, Y. Wang, S. Wang, L. Yu, C. Ma, D. Deng and X. Bao,
242 *Energy Environ. Sci.*, 2020, **13**, 119-126.

243 2 R. Chen, H. Y. Su, D. Liu, R. Huang, X. Meng, X. Cui, Z. Q. Tian, D. H. Zhang and D. Deng,
244 *Angew. Chem. Int. Ed.*, 2020, **59**, 154-160.

245